

Exploring the recovery capacity of recycling agents on atomic-scale energy properties of aged bitumen and their potential correlations with high-temperature rheological performance

Ren, Shisong; Liu, Xueyan; Erkens, Sandra

DOI

[10.1016/j.matdes.2024.112957](https://doi.org/10.1016/j.matdes.2024.112957)

Publication date

2024

Document Version

Final published version

Published in

Materials & Design

Citation (APA)

Ren, S., Liu, X., & Erkens, S. (2024). Exploring the recovery capacity of recycling agents on atomic-scale energy properties of aged bitumen and their potential correlations with high-temperature rheological performance. *Materials & Design*, 241, Article 112957. <https://doi.org/10.1016/j.matdes.2024.112957>

Important note

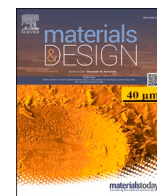
To cite this publication, please use the final published version (if applicable).
Please check the document version above.

Copyright

Other than for strictly personal use, it is not permitted to download, forward or distribute the text or part of it, without the consent of the author(s) and/or copyright holder(s), unless the work is under an open content license such as Creative Commons.

Takedown policy

Please contact us and provide details if you believe this document breaches copyrights.
We will remove access to the work immediately and investigate your claim.



Exploring the recovery capacity of recycling agents on atomic-scale energy properties of aged bitumen and their potential correlations with high-temperature rheological performance

Shisong Ren^{*}, Xueyan Liu, Sandra Erkens

Section of Pavement Engineering, Delft University of Technology, Netherlands

ARTICLE INFO

Keywords:

Rejuvenated bitumen
Atomic-scale energy indices
Molecular dynamics simulation
High-temperature performance
Potential correlations

ABSTRACT

This study implements molecular dynamics (MD) simulations to explore the atomic-level energy properties of rejuvenated bitumen, considering the influence of different recycling agent (RA) types, dosages and aging levels of bitumen. Moreover, the potential correlations between energy indices and high-temperature performance of rejuvenated bitumen are explored. Our findings show that recycling agents can effectively reinstate the cohesive energy density (CED) values of aged bitumen, correlating well with their high-temperature rheological properties. The results reveal that the energy parameters of potential energy (U_{VEP}), kinetic energy (U_{WEK}), non-bond energy (E_N), total energy (U_{VET}), diagonal energy (U_{NED}), and cross-terms energy (E_{CT}) can reflect the restoration level of recycling agents (RAs) on atomic-level energy characteristics of aged bitumen. Compared to rutting failure temperature (RFT), elastic recovery ($R_{3,2}$), and creep compliance ($J_{nr3,2}$), the zero-shear viscosity (ZSV) greatly correlates with CED. Meanwhile, the U_{WEK} index from MD simulations demonstrates a strong correlation with high-temperature rheological indicators of rejuvenated bitumen. With the rise in U_{WEK} , there is a linear decrease in the RFT, $\text{Log}(ZSV)$, and $R_{3,2}$ values of rejuvenated bitumen. Conversely, the $\text{Log}(J_{nr3,2})$ exhibits a linear increasing trend. However, the correlation patterns between rheological indicators and either E_N or E_{CT} are contingent on the aging degree of bitumen. Based on the correlation coefficient, the U_{WEK} stands out as the primary choice among all energy indices for predicting high-temperature rheological performance of rejuvenated bitumen.

1. Introduction

The Netherlands' Sustainable Road Pavement Transition Path targets climate neutrality and full circularity in road construction. It emphasizes high-quality material recycling, aiming for a 50 % reduction in primary raw resource use, without compromising quality standards [1]. The goal of this sustainability approach is to reuse about 70 % of reclaimed porous asphalt waste materials by the year 2030 [2]. To ensure that recycled asphalt pavement with a high reclaimed asphalt pavement (RAP) ratio performs adequately, the adoption of recycling agents (RAs) is crucial [3,4]. Thus, it becomes imperative to develop efficient recycling techniques, though challenges persist, particularly in the inconsistent assessment methods of recovery effectiveness and the unclear mechanisms underlying RAs' interactions with aged bitumen, which are strongly related to the difference in chemical composition of various RAs [5].

However, relying solely on macroscopic tests for the design, production, and evaluation framework of recycling agent-aged bitumen blends is inadequate [6]. The diverse composition of both the recycling agent (RA) and aged bitumen necessitates comprehensive rheological and mechanical testing [7]. In response to this, scientists have engaged in molecular-level characterizations and simulations of various rejuvenated bitumen systems [8,9]. Molecular dynamics (MD) simulations have emerged as a popular tool for delving into the fundamental efficiency and mechanisms of various rejuvenated bitumen scenarios.

The restoration effects of different RA molecules on thermodynamic properties were studied using MD simulations, including the waste cooking oil [10], single component $C_{12}H_{16}$ [11], poly-sulfide [12], paraffin [13], straight-chain and aromatic recycling agents [14]. Most studies demonstrated the ability of these RAs to restore molecular-level indicators, encompassing density, glass transition temperature, cohesive energy density, free energy, diffusion coefficient, and fractional free

^{*} Corresponding author.

E-mail address: Shisong.Ren@tudelft.nl (S. Ren).

<https://doi.org/10.1016/j.matdes.2024.112957>

Received 3 October 2023; Received in revised form 13 April 2024; Accepted 17 April 2024

Available online 18 April 2024

0264-1275/© 2024 The Author(s). Published by Elsevier Ltd. This is an open access article under the CC BY license (<http://creativecommons.org/licenses/by/4.0/>).

volume [15–18]. Nevertheless, the heterogeneity of RA compositions and thermodynamic metrics complicates the identification of effective molecular-level parameters for assessing softening efficiency across different RAs [19,20]. It was reported that the Rej-Hybrid rejuvenator with heightened polarity, meticulously crafted from a well-balanced blend of proteins, lipids, and nucleic acids, exhibited superior adsorption on a siliceous surface and lower moisture susceptibility [21]. Furthermore, the limited integration of MD simulation findings with rheological and mechanical data obtained from experiments has led to a disconnect between theoretical research and practical engineering in the field of rejuvenated bitumen [22,23].

The main objective of this study is to fundamentally understand the recovery capacity of different recycling agents (RAs) on the high-temperature performance of aged bitumen at the molecular scale. The aim is to incorporate thermodynamic parameters derived from molecular dynamics simulations, establishing a close correlation with extensive critical rheological data obtained through experiments. The research framework is depicted in Fig. 1. The molecular models of rejuvenated bitumen with variable RA types/dosages and aging levels of bitumen will be established to output the thermodynamic parameters. The feasibility of these thermodynamic parameters for effectively evaluating and distinguishing the restoration efficiency of various RAs will be estimated. Additionally, we'll measure critical high-temperature properties like RFT, ZSV, $R_{3.2}$, and $J_{nr3.2}$ of rejuvenated bitumen using rheological tests. Finally, the potential links between these thermodynamic indices and critical rheological indicators of rejuvenated bitumen are explored.

2. Materials and experimental tests

2.1. Materials and sample preparation

In this study, 70/100 fresh bitumen was utilized to prepare aged and rejuvenated binders, and its basic properties are listed in Table 1. Meanwhile, four types of recycling agents (RAs) within different categories were used and named bio-oil (B), engine-oil (E), naphthenic-oil (N), and aromatic-oil (A). Their physical and chemical properties are shown in Table 2.

The fresh bitumen was treated with short- and long-term aging procedures by the Thin Film Oven test (TFOT) and Pressure Aging Vessel (PAV). The temperature and aging time in TFOT test were 163 °C and 5 h, while temperature and pressure in the PAV test were 100 °C and 2.1

Table 1

The properties of fresh 70/100 bitumen.

Items	Properties	Value	Test standard
Physical indicators	Density (25 °C, g/cm ³)	1.017	EN 15326
	Penetration (25 °C, 1/10 mm)	91	ASTM D35
	Softening point (°C)	48.0	ASTM D36
	Viscosity (135 °C, Pa·s)	0.80	AASHTO T316
Element analysis	Carbon C (wt%)	84.06	ASTM D7343
	Hydrogen H (wt%)	10.91	
	Nitrogen N (wt%)	0.90	
	Oxygen O (wt%)	0.62	
	Sulfur S (wt%)	3.52	
SARA fractions	Asphaltene As (wt%)	12.8	ASTM D4124
	Resin R (wt%)	30.3	
	Aromatic A (%)	53.3	
	Saturate S (%)	3.6	
Mechanical properties (60 °C, 1.6 Hz)	Complex modulus G* (kPa)	2.4	AASHTO M320
	Phase angle δ (°)	84.5	

Table 2

The physical and chemical indicators of four recycling agents.

	Recycling agents	Bio-oil	Engine-oil	Naphthenic-oil	Aromatic-oil
Physical	Density (25 °C, g/cm ³)	0.911	0.833	0.875	0.994
	Viscosity (25 °C, cP)	50	60	130	63,100
	Flash point (°C)	265–305	>225	>230	>210
Chemical	Nitrogen N (%)	0.15	0.23	0.12	0.55
	Carbon C (%)	76.47	85.16	86.24	88.01
	Hydrogen H (%)	11.96	14.36	13.62	10.56
	Sulfur S (%)	0.06	0.13	0.10	0.48
	Oxygen O (%)	11.36	0.12	0.10	0.40
	M _n (g/mol)	286.4	316.5	357.1	410.0

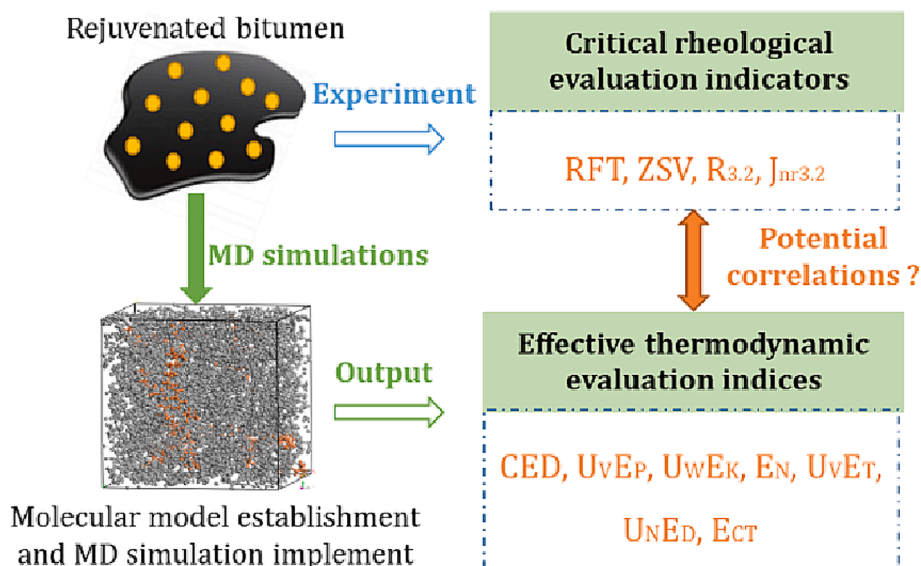


Fig. 1. Flowchart of research structure.

MPa, respectively. The long-term aging time varied from 20 h to 40 h and 80 h, and the aged bitumen was abbreviated with 1P, 2P, and 4P. Meanwhile, the virgin and TFOT-aged bitumen are labelled as VB and SAB.

Three aged bitumen (1P, 2P, and 4P) were firstly preheated to 160 °C, and four recycling agents (labelled as B, E, N, and A) were blended for 10 min to manufacture the rejuvenated bitumen. For 2P aged bitumen, the recycling agent (RA) dosage increases from 5 % to 15 % with an interval of 2.5 %. Meanwhile, the RA content in both 1P and 4P binders was 10 % to see the effect of bitumen aging level. The bio-oil, engine-oil, naphthenic-oil, and aromatic-oil rejuvenated bitumen groups are labelled as BORB, EORB, NORB, and AORB. Moreover, the abbreviation of each rejuvenated bitumen considers the aging level of bitumen and RA dosage. For instance, the 2P10B rejuvenated bitumen was prepared by adding a 10 % bio-oil to 2P aged bitumen.

2.2. Experimental tests

The high-temperature temperature sweeps and flow tests were conducted to measure the rutting failure temperature (RFT) and zero-shear viscosity (ZSV) of rejuvenated bitumen. Meanwhile, the multiple stress creep and recovery (MSCR) test was performed to determine the recovery percentage ($R_{3,2}$) and creep compliance ($J_{cr,3,2}$). Comprehensive details regarding test conditions and the elucidation of these crucial indicators can be located in our prior research [24].

2.3. Restoration percentage (TRP) calculation

In order to quantitatively assess the impact of diverse conditions, including recycling agent type, dosage, and bitumen aging degree, on the molecular-scale properties of aged bitumen, the restoration percentage (TRP) for various rejuvenated bitumen models is calculated using Eq.1 based on thermodynamic property results obtained from MD simulations.

$$TRP = \frac{T_{aged} - T_{rejuvenated}}{T_{aged} - T_{fresh}} * 100 \quad (1)$$

where TRP is the restoration percentage based on MD simulation outputs, and T shows the thermodynamic parameters, including the density, cohesive energy density, and energy parameters. Moreover, T_{aged} , $T_{rejuvenated}$, and T_{fresh} are the thermodynamic properties of aged, rejuvenated, and fresh bitumen, respectively.

3. Molecular dynamics simulations on rejuvenated bitumen

To mitigate any potential impact stemming from the MD simulation protocol, the methods for generating rejuvenated bitumen is consistent with the approach for aged binders, as described in [25]. The molecular models of aged bitumen were established based on measured chemical characteristics, such as saturate, aromatic, resin, asphaltene (SARA) fractions, functional group distribution, element composition, and molecular weight distribution [26]. These molecular models of aged bitumen agree well with other work showing the ratio of polar components to nonpolar ones in oxidized bitumen is higher than in virgin asphalt [27]. As shown in Fig. 2(a), recycling agent (RA) molecules (in orange) were randomly dispersed among the aged bitumen molecules (in grey). Subsequently, an initial model geometry optimization was executed to achieve energy minimization and configuration stabilization. This is followed by a condensed simulation under the isothermal isobaric (NPT) ensemble using the COMPASSII force field to attain the pre-equilibrium state, which is the first forcefield derived from an ab initio calculation method and the most popular forcefield to bituminous materials [11–15]. During the NPT process, intermolecular forces foster mutual molecular attraction. After NPT, the pre-equilibrium model underwent a secondary equilibrium phase with the canonical (NVT) ensemble, thereby fostering enhanced interaction between the RA and aged bitumen molecules. Throughout both NPT and NVT simulations, a time step of 1 fs (fs) and a total runtime of 200 picoseconds (ps) were adopted. Pressure and temperature control during MD simulations were facilitated through the employment of the Anderson barostat and Nose thermostat, respectively. The van der Waals intermolecular force was computed using the Atom-based method, employing a cut-off distance of 12.5 Å, while electrostatic interactions were determined via the Ewald method.

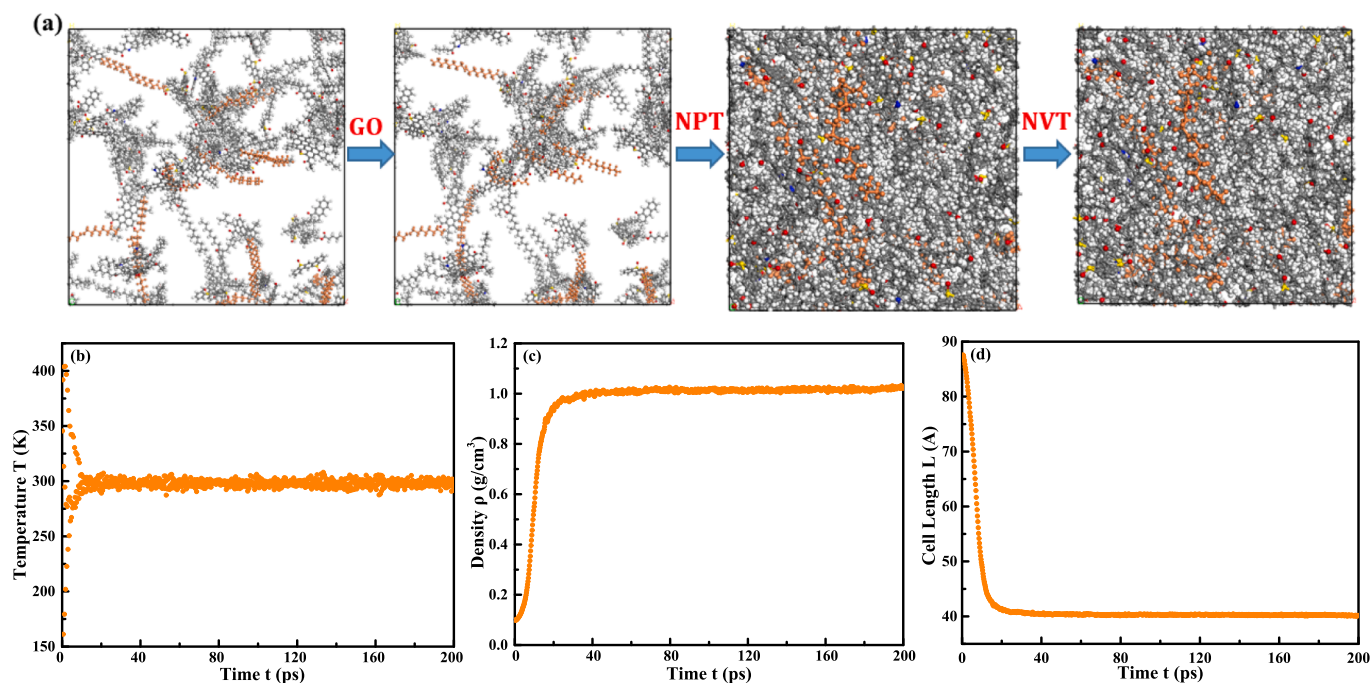


Fig. 2. Graph illustration of MD model establishment of rejuvenated bitumen and thermodynamic parameters' variations during MD simulations (a) MD simulation process; (b) Temperature, (c) Density, and (d) Cell Length during NPT.

Throughout both NPT and NVT simulations, continuous monitoring of the rejuvenated bitumen model involved real-time evaluation of energy, temperature, and density parameters, thereby ensuring the convergence of the simulation process. Fig. 2 presents a selection of overarching outcomes. Notably, in the NPT simulation, equilibrium states for temperature ($T = 298$ K), density (ρ), cell length (L), and energy parameters (potential, kinetic, non-bond, and total energies) were promptly achieved. This substantiates the stability and precision of the MD simulation protocol.

Within this study, 28 rejuvenated bitumen models with variable recycling agent type, dosage, and aging degree of bitumen were subjected to the MD simulations, and their MD simulation protocols were the same as discussed above. The model information of these samples is listed in Table 3. In this study, the molecular model preparation for each rejuvenated bitumen is conducted independently, using identical MD simulation setups (including the forcefield, relaxation time, time step, etc.). When considering the temperature factor, the molecular models of rejuvenated bitumen will be reconstructed in MD simulations with NPT and NVT ensembles at various temperatures to eliminate the influence of initial molecular structures.

The investigation encompasses three aging degrees (1P, 2P, and 4P) of bitumen, corresponding to prolonged aging durations of 20, 40, and 80 h, delving into the molecular constituents within differently aged bitumen models. Additionally, the average molecular structures of various RAs are introduced in our previous work [25], including the bio-oil (B), engine-oil (E), naphthenic-oil (N), and aromatic-oil (A). Moreover, the sample name also contains the RA dosage. For 2P aged bitumen, five RA dosages (5 %, 7.5 %, 10 %, 12.5 %, and 15 %) of four RAs are considered. However, for 1P and 4P aged binders, only the 10 % dosage was used, providing insights into the relationship between aging levels and properties of rejuvenated bitumen.

Achieving equilibrium molecular configurations for various rejuvenated binders involves following the sequence of Geometry Optimization (GO), Isothermal Isobaric (NPT), and Canonical (NVT) simulations. Fig. 3 presents the ultimate equilibrium structures of 2P rejuvenated bitumen at 298 K, featuring varying RA dosages of 5 %, 10 %, and 15 %. It is worth noting that MD simulations for all rejuvenated bitumen models encompass a range of temperatures (273 K, 298 K, 333 K, and 393 K) to evaluate the temperature sensitivity of predicted properties of rejuvenated bitumen. Consequently, both NPT and NVT simulations are redone for each model across these distinct temperatures. In Fig. 3, aged bitumen molecules are shown in grey color, while other bright colors indicate the different RA molecules (Orange: bio-oil; Blue: engine-oil; Pink: naphthenic-oil; Green: aromatic-oil). Notably, the distribution of RA molecules in aged bitumen is uneven, influenced by both RA type and dosage. Our prior studies [25,28] have validated the molecular dynamics (MD) simulation outcomes for both aged bitumen and RAs, establishing a foundation for the dependability of MD results for rejuvenated binders in the current study.

4. MD simulation results and discussion

4.1. Cohesive energy density CED

The cohesive energy density E_{CED} can examine the mutual attractiveness of all molecules per unit volume, calculated as follows:

$$E_{CED} = E_{coh}/V \quad (2)$$

where E_{coh} is the total cohesive energy of the whole bitumen model (J), and V shows the model volume (cm^3).

The CED-based restoration percentages CEDR values of different rejuvenated bitumen are calculated and displayed in Fig. 4. The CEDR values of all rejuvenated bitumen enlarge linearly as the RA dosage increases. Regardless of temperature and RA dosage, the CEDR values of BORB and AORB are lower than EORB and NORB binders. It means that the aromatic-oil shows the lower regenerating effect on the CED parameter of aged bitumen, while the naphthenic-oil has the largest CEDR values. However, it was shown that the recycling agent with pyrene and fluoranthene molecules reduced the asphaltene agglomeration in aged bitumen through disrupting the π -stacked structure of asphaltenes based on the Density Functional Theory (DFT) studies [29,30]. The aromatic-oil with similar structure would show detaching effect on aggregated asphaltene clusters, which should be validated in future work [29,30].

Simultaneously, the restoration capacity of bio-oil and engine oil on the CED recovery of aged bitumen falls in the middle range, with the engine oil exerting a more pronounced influence compared to the bio-oil. Temperature shows a positive impact on enlarging the CEDR values of rejuvenated bitumen. At both 273 K and 298 K, all CEDR values are lower than 100 %, indicating that all recycling agents fail to regenerate the CED value of aged bitumen to virgin bitumen level. Within all temperature and RA dosage regions, the CEDR values of engine-oil, bio-oil, and aromatic-oil rejuvenated bitumen are lower than 100 %. Therefore, most RAs cannot completely restore the cohesive energy density of aged bitumen even through their RA content reaches 15 %. In general, the CED parameter proves effective in discerning the restoration effect between aromatic oils and other substances. While variations in the CEDR of different rejuvenated bitumen are noticeable, the magnitude of CEDR values for bio-oil, engine oil, and naphthenic oil contradicts their order in high-temperature properties observed in experimental tests. The CED parameter can influence, but only to a limited extent, the reflection of the restoration potentials of various recycling agents on the macroscale high-temperature performance of aged bitumen.

4.2. Energy parameters of rejuvenated bitumen

At the atomic level, diverse energy parameters influence the bitumen model, influencing its macroscale performance. Simultaneously, these energy parameters serve as the foundation for calculating various thermodynamic properties of bitumen models. With the COMPASSII

Table 3
Potential energy-based restoration percentages of rejuvenated bitumen.

E_pR	BORB	EORB	NORB	AORB	U_pE_pR	BORB	EORB	NORB	AORB
5.0 %	-10.6	4.69	1.54	-90.7	5.0 %	54.6	65.3	52.7	-33.1
7.5 %	-6.63	8.08	2.05	-125	7.5 %	76.3	98.3	88.0	-46.6
10.0 %	-5.52	11.79	2.11	-179	10.0 %	113	141	114	-56.4
12.5 %	-4.40	14.21	5.73	-231	12.5 %	145	175	148	-66.7
15.0 %	-3.91	18.53	6.34	-281	15.0 %	176	204	184	-72.1
U_wE_pR	BORB	EORB	NORB	AORB	U_NE_pR	BORB	EORB	NORB	AORB
5.0 %	74.9	93.5	86.6	-70.6	5.0 %	58.4	65.6	53.7	-24.7
7.5 %	114	139	132	-92.9	7.5 %	89.5	95.7	81.5	-32.0
10.0 %	159	194	176	-129	10.0 %	119	132	108	-44.3
12.5 %	203	245	224	-161	12.5 %	149	164	136	-54.5
15.0 %	249	284	262	-187	15.0 %	179	188	158	-62.4

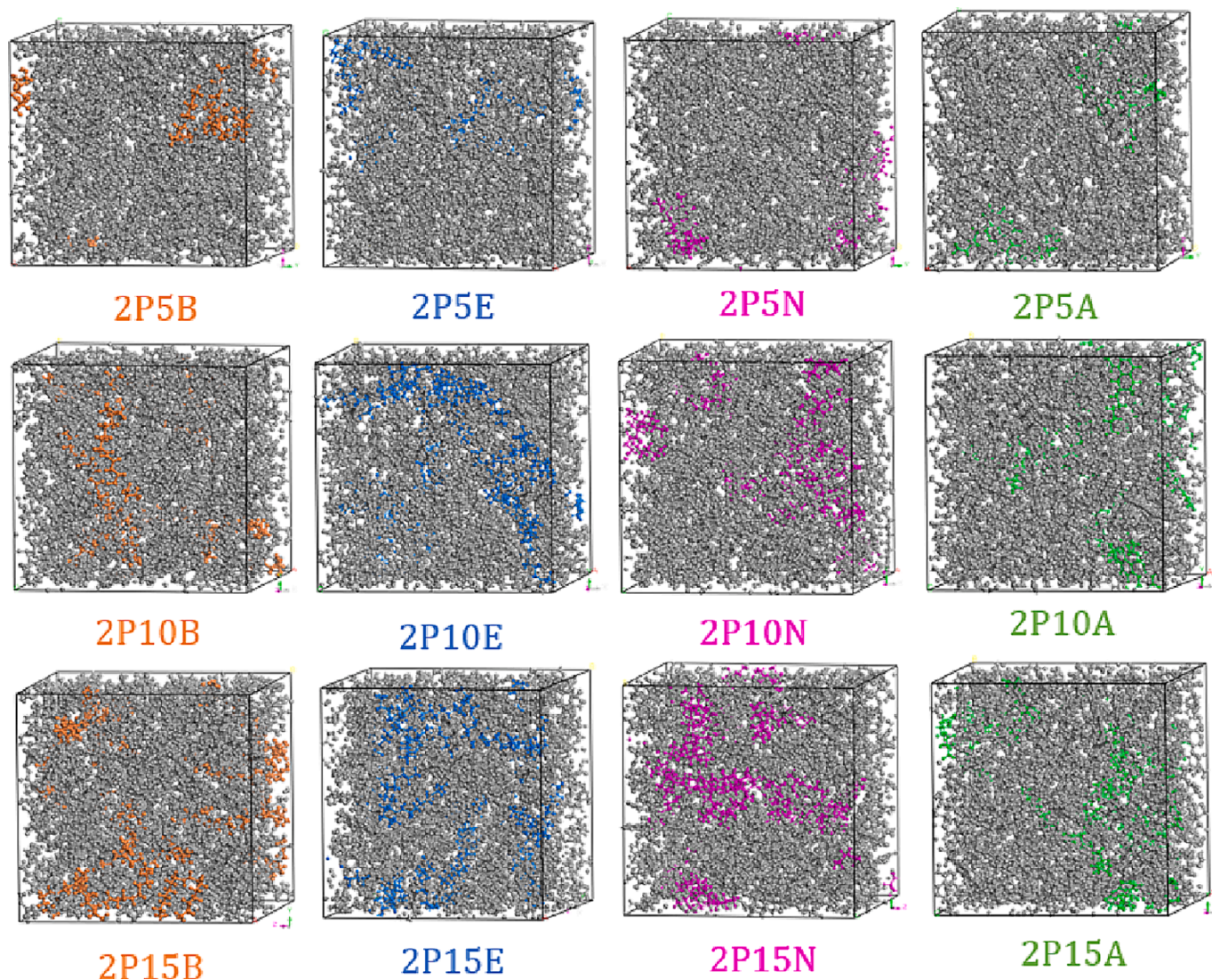


Fig. 3. Bulk molecular models of 2P5, 2P10, and 2P15 rejuvenated bitumen at 298 K Grey: aged bitumen; Orange: bio-oil; Blue: engine-oil; Pink: naphthenic-oil; Green: aromatic-oil. (For interpretation of the references to color in this figure legend, the reader is referred to the web version of this article.)

force field, various energy parameters show the relationships below:

$$E_T = E_P + E_K = (E_V + E_N) + E_K = [(E_D + E_{CT}) + E_N] + E_K \quad (3)$$

where E_T is the total energy of the whole rejuvenated bitumen model, composed of potential energy E_P and kinetic energy E_K . Meanwhile, the two elements of potential energy are valence energy E_V and non-bond energy E_N . The valence energy is divided into diagonal energy E_D and cross-terms energy E_{CT} . Further, diagonal energy contains bond energy, angle energy, torsion energy, and inversion energy, while cross-terms energy has different terms, such as stretch-stretch energy, stretch-bond-stretch energy, etc. Generally, non-bond energy contains van der Waals energy, electrostatic energy, and hydrogen energy. Discussing and comparing all energy terms across various rejuvenated bitumen models presents a challenge. This study focuses on examining only six primary energy parameters (potential energy, kinetic energy, non-bond energy, total energy, diagonal energy, and cross-terms energy). These energy parameters of rejuvenated bitumen models are obtained as output from molecular dynamics equilibrium simulations conducted with NPT and NVT ensembles.

Several average energy parameters of rejuvenated bitumen models are computed to evaluate the recovery potential concerning energy characteristics, albeit to a lesser extent: (i) Volume-average energy pa-

rameters $U_V E$; (ii) Weight-average energy parameters $U_W E$; and (iii) Number-average energy parameters $U_N E$. These unit energy parameters are obtained following Eqs. (4)–(6).

$$U_V E = \frac{E}{V} \quad (4)$$

$$U_W E = \frac{E}{W} \quad (5)$$

$$U_N E = \frac{E}{N} \quad (6)$$

where E is the energy parameter of rejuvenated bitumen; V , W , and N refer to the model volume, molecular weight, and molecular number of the whole bitumen model, respectively. The unit of $U_V E$ is kcal/(mol·Å³), while the unit of $U_W E$ and $U_N E$ is the same as kcal/mol.

This investigation explores the effectiveness of energy parameters derived from molecular dynamics (MD) simulations in indicating the recovery performance of recycling agents (RAs) on aged bitumen. Given the heterogeneous nature of bitumen molecular distribution, the energy parameters within a bitumen model exhibit non-uniformity. Consequently, diverse forms of expression for energy parameters are employed to examine the impacts of aging and adding recycling agents,

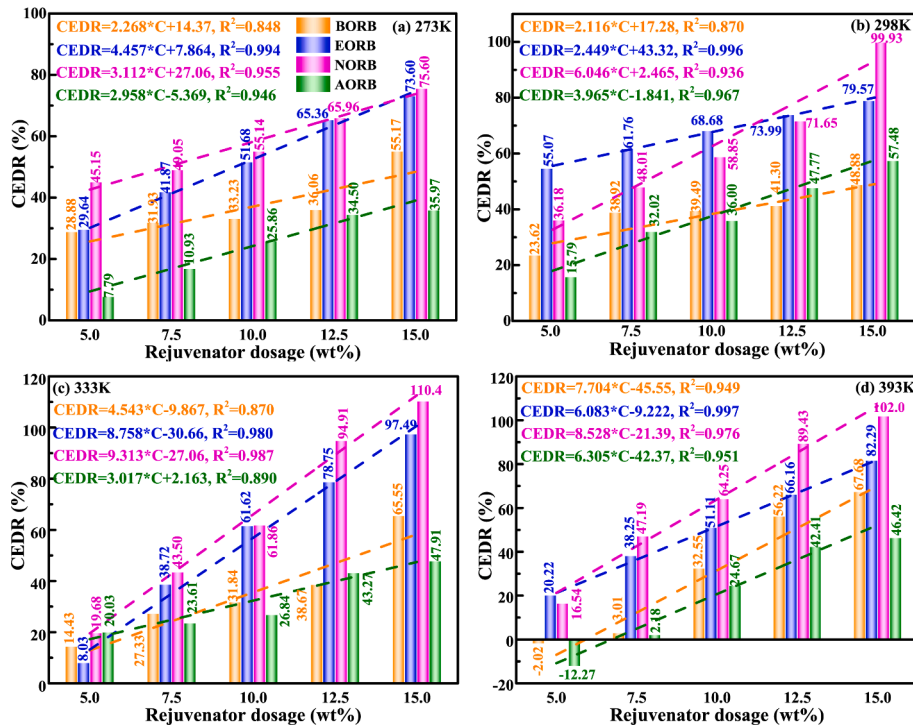


Fig. 4. The CEDR values versus RA dosage of different rejuvenated bitumen.

including the energy of whole model E, energy per volume $U_V E$, energy per weight $U_W E$, and energy per number $U_N E$.

It is observed that for one specific energy, more than one index can effectively assess the restoration level, such as kinetic energy E_K and $U_W E_K$, and it is necessary to further determine the critical energy parameters according to the restoration percentages calculated following Eq. (1). Table 3 lists the potential energy-based restoration percentages of rejuvenated bitumen. All $E_P R$ values of AORB binders are negative, indicating that the addition of aromatic-oil fails to restore the potential energy of aged bitumen. Conversely, the other three recycling agents (bio-oil, engine-oil, and naphthenic-oil) exhibit a positive recovery effect, and their $E_P R$ values enlarge significantly as the RA dosage increases. However, the $E_P R$ values of rejuvenated bitumen are lower than $U_V E_P R$, $U_W E_P R$, and $U_N E_P R$ values. This is because the quantity of recycling agent (RA) molecules is constrained by the entirety of aged bitumen molecules, resulting in a comparatively low impact on the overall potential energy. Nevertheless, the recovery effect of RA molecules on aged bitumen per unit volume, weight, and number is more pronounced. In addition, the $E_P R$ values of BORB are negative due to the strong intermolecular interaction between polar groups in bio-oil with aged bitumen molecules, but the positive effect of bio-oil on unit potential energy is observed. Regardless of RA dosage and unit potential energy type, engine-oil has the largest restoration efficacy on potential

energy, followed by NORB, BORB, and AORB. Further, the $U_W E_P R$ values are higher than $U_V E_P R$ and $U_N E_P R$, and the latter two are close, which are higher than the restoration percentages based on critical high-temperature indicators. To this end, the $U_V E_P R$ index with the lowest values is recommended to be adopted for evaluating the restoration levels of bio-oil, engine-oil, and naphthenic-oil on the potential energy of aged bitumen.

The kinetic energy-based restoration percentages $E_K R$ of rejuvenated bitumen are shown in Table 4. It further reveals the unsuitability of $U_V E_K$ and $U_N E_K$ indices for restoration efficiency evaluation because the negative effect of recycling agent (RA) dosage is observed based on $U_V E_K R$ and $U_N E_K R$ results. Besides, the $E_K R$ values are much higher than the $U_W E_K R$, and the former (400–1700 %) seriously deviated from the sequence order of restoration percentages based on critical macroscale performance [24]. Thus, the $U_W E_K R$ acts as the critical index for assessing the restoration efficiency of different RAs on the kinetic energy of aged bitumen. By comparing the magnitude of different $E_K R$, the influence level of recycling agents on E_K and $U_N E_K$ is more significant than the $U_V E_K$ and $U_W E_K$. Further, all $U_W E_K R$ values of rejuvenated bitumen are lower than 100 %, indicating that the weight-average kinetic energy of aged bitumen cannot be fully regenerated by adding RAs even when the RA dosage reaches 15 %. The sequence of $U_W E_K R$ values of rejuvenated bitumen follows EORB > NORB > BORB > AORB.

Table 4
Kinetic energy-based restoration percentages of rejuvenated bitumen.

$E_K R$	BORB	EORB	NORB	AORB	$U_V E_K R$	BORB	EORB	NORB	AORB
5.0 %	449	513	481	456	5.0 %	29.5	31.2	67.5	24.4
7.5 %	733	761	759	631	7.5 %	5.13	25.2	59.4	12.8
10.0 %	943	1089	1035	893	10.0 %	-9.40	12.4	55.1	-8.97
12.5 %	1226	1418	1311	1158	12.5 %	-29.9	2.99	43.2	-26.5
15.0 %	1511	1669	1589	1417	15.0 %	-39.7	-8.97	1.71	-54.3
$U_W E_K R$	BORB	EORB	NORB	AORB	$U_N E_K R$	BORB	EORB	NORB	AORB
5.0 %	17.1	26.3	22.1	10.2	5.0 %	-3050	-1505	15.3	-577
7.5 %	25.0	36.9	32.6	12.6	7.5 %	-5171	-2379	-217	-977
10.0 %	30.1	49.9	42.1	16.0	10.0 %	-6716	-3508	-494	-1539
12.5 %	37.0	62.2	51.1	19.6	12.5 %	-8540	-4523	-731	-2003
15.0 %	43.8	71.8	59.9	22.2	15.0 %	-10186	-5125	-928	-2542

It was concluded that only E_N parameter could reflect the recovery level of all RAs on non-bond energy of aged bitumen, while other unit E_N parameters fail to evaluate the restoration efficiency of aromatic-oil rejuvenated bitumen. This finding is further verified based on the restoration percentages results presented in Table 5. The U_{VE_NR} , U_{WE_NR} , and U_{NE_NR} values of all rejuvenated binders are located in -20 – 20 %, lower than the E_NR region (0 – 51 %). It is evident that the extent of recycling agents' impact on the average non-bond energy per unit volume, weight, and number is constrained and less than that on potential and kinetic energy. The E_NR values of rejuvenated bitumen are reasonable although it is smaller than the restoration percentages based on rheological and mechanical properties. Similar to U_{WE_K} , the E_N value of aged bitumen does not return to the virgin bitumen level by adding RAs with dosages varying from 5 % to 15 %. Furthermore, the BORB shows the highest E_NR value, followed by EORB and NORB, while aromatic-oil exhibits the lowest recovery efficacy on non-bond energy of aged bitumen.

The restoration percentages based on the total energy of rejuvenated binders are displayed in Table 6. All restoration percentages of AORB binders show a decreasing trend as the aromatic-oil dosage increases, but the positive U_{VE_T} , U_{WE_T} , and U_{NE_T} values of AORB binders are observed. This suggests that introducing aromatic oil can recover the total energy of aged bitumen, but this rejuvenating effect diminishes with an increase in aromatic oil dosage. This contrasts with the potential energy outcome, where aromatic oil is unable to restore all potential energy terms of aged bitumen. Meanwhile, the E_T values of AORB binders are negative, indicating that adding aromatic-oil shows a negative effect on the total energy of the whole aged bitumen model. However, it can restore the average total energy. Similar to potential energy, the U_{VE_T} , U_{WE_T} , and U_{NE_T} indicators can evaluate the restoration efficiency of bio-oil, engine-oil, and naphthenic-oil on the total energy of the aged bitumen model. The U_{WE_T} values are higher than the U_{VE_T} and U_{NE_T} , larger than the macroscale restoration efficiency. The influence level of these RAs on the weight-average total energy is more significant than the volume-average and number-average ones. Moreover, the U_{VE_T} and U_{NE_T} values are similar, and the U_{VE_T} parameter is selected as an evaluation index for the total energy term to be consistent with potential energy. The order of U_{VE_T} values of rejuvenated bitumen is $EORB > NORB \approx BORB > AORB$.

Additionally, the diagonal energy-based restoration percentages E_{DR} of rejuvenated bitumen are summarized in Table 7. The E_{DR} and $U_{WE_{DR}}$ values of BORB, EORB, and NORB binders decrease remarkably as the RA dosage increases. Thus, the E_D and U_{WE_D} parameters are not effective evaluation energy indicators. With the U_{VE_D} and U_{NE_D} indices, the restoration efficiency of bio-oil, engine-oil, and naphthenic-oil on the diagonal energy can be evaluated, but they fail to assess the effectiveness of aromatic-oil because the $U_{VE_{DR}}$ and $U_{NE_{DR}}$ values of AORB have a negative correlation with aromatic-oil dosage, although low aromatic-oil content (5 %, 7.5 %, and 10 %) can restore the U_{VE_D} and U_{NE_D} values of aged bitumen to a certain degree. Interestingly, it is observed that the order of magnitude for $U_{VE_{DR}}$, $U_{WE_{DR}}$, and $U_{NE_{DR}}$ is larger than

E_{DR} , indicating the recovery effect on unit diagonal energy of the aged bitumen model is more significant than the whole model. This phenomenon is opposite to the non-bond energy case. The $U_{VE_{DR}}$ and $U_{NE_{DR}}$ values of BORB, EORB and NORB are much higher than their restoration percentages on critical high-temperature properties (0 – 200 %). To narrow the gap, the smaller one (U_{NE_D}) parameter is proposed as an effective index for estimating the restoration efficiency of bio-oil, engine-oil, and naphthenic-oil on the diagonal energy term of aged bitumen model.

The restoration percentages based on cross-terms energy of rejuvenated bitumen E_{CTR} are demonstrated in Table 8. It is detected that the $U_{VE_{CTR}}$, $U_{WE_{CTR}}$, and $U_{NE_{CTR}}$ values of all rejuvenated binders are negative, implying that the involvement of all recycling agents (RAs) has no recovery potential on the volume, weight, and number-average cross-terms energy of aged bitumen. However, the E_{CTR} index exhibits an opposite result, and thus E_{CT} parameter is the only valid indicator to appraise the recovery efficacy of RAs on cross-terms energy on aged bitumen. Further, the E_{CTR} values of all rejuvenated binders are lower than 25 %, showing that these RAs (even with a 15 % RA dosage) have restricted recoverable effects on the cross-terms energy of aged bitumen. The sequence of E_{CTR} values of rejuvenated bitumen is $AORB > BORB > EORB > NORB$.

The flexibility of various energy parameters as effective indicators for evaluating the recovery efficiency of different RAs is discussed. Table 9 summarizes the effect of aging and adding recycling agents (RAs) on these energy parameters of bitumen. Regardless of evaluation size, all potential energy indicators (E_P , U_{VE_P} , U_{WE_P} , and U_{NE_P}) can evaluate the recovery potential of bio-oil, engine-oil, and naphthenic-oil, but fail to assess the aromatic-oil. The E_K and U_{WE_K} indices are applicable to estimate the restoration effect on the kinetic energy of aged bitumen. Regarding the non-bond energy, the E_N is an effective evaluation parameter, while the others cannot succeed in the aromatic-oil rejuvenated binder. Meanwhile, it is not possible to use the E_T index for restoration efficiency evaluation on the total energy of aged bitumen. The three average parameters (U_{VE_T} , U_{WE_T} , and U_{NE_T}) show the limitation in assessing the aromatic-oil rejuvenated bitumen. In addition, the diagonal energy is in the same situation as the total energy and only E_{CT} can reflect the restoration level on cross-term energy. Overall, the effective energy parameters for all RAs are E_K (U_{WE_K}), E_N , and E_{CT} . Three additional energy parameters (potential, total, and diagonal) play a crucial role in defining the thermodynamic and mechanical characteristics of rejuvenated bitumen. The only limitation for these parameters lies in their application with aromatic-oil. Consequently, this study also aims to put forth effective potential, total, and diagonal energy parameters specifically tailored for bio-oil, engine-oil, and naphthenic-oil rejuvenated binders.

Eventually, the critical energy indicators for effectively evaluating the restoration efficiency are proposed: U_{VE_P} , U_{WE_K} , E_N , U_{VE_T} , U_{NE_D} , and E_{CT} . These restoration percentages based on critical energy parameters of different rejuvenated bitumen with 15 % RA dosage are plotted in Fig. 5. These critical energy indicators can reflect the recovery

Table 5
Non-bond energy-based restoration percentages of rejuvenated bitumen.

E_{NR}	BORB	EORB	NORB	AORB	$U_{VE_{NR}}$	BORB	EORB	NORB	AORB
5.0 %	14.4	17.4	13.3	3.43	5.0 %	2.65	4.93	−4.20	−7.39
7.5 %	15.4	20.3	16.0	6.77	7.5 %	4.74	−2.37	−1.46	−7.66
10.0 %	35.3	25.1	24.3	8.44	10.0 %	8.94	−1.46	−0.36	−13.1
12.5 %	43.0	36.4	30.5	9.96	12.5 %	11.0	0.18	0.82	−15.6
15.0 %	50.7	41.4	33.5	19.8	15.0 %	13.1	1.64	2.46	−17.7
$U_{WE_{NR}}$	BORB	EORB	NORB	AORB	$U_{NE_{NR}}$	BORB	EORB	NORB	AORB
5.0 %	4.47	3.77	3.43	−5.41	5.0 %	−1.27	−8.37	−6.63	−8.48
7.5 %	6.31	5.06	1.14	−5.91	7.5 %	−0.13	−5.73	−4.46	−9.71
10.0 %	12.2	6.60	3.33	−9.14	10.0 %	3.20	−4.09	−3.08	−14.5
12.5 %	15.7	7.50	3.77	−12.3	12.5 %	4.19	−1.42	−2.20	−16.3
15.0 %	18.9	7.55	1.84	−9.19	15.0 %	5.00	2.69	1.12	−19.1

Table 6

Total energy-based restoration percentages of rejuvenated bitumen.

E _T R	BORB	EORB	NORB	AORB	U _V E _T R	BORB	EORB	NORB	AORB
5.0 %	26.9	29.4	29.0	−21.3	5.0 %	77.2	81.4	72.8	28.8
7.5 %	13.3	22.6	19.1	−46.1	7.5 %	87.5	99.8	93.1	20.7
10.0 %	8.97	13.3	9.82	−85.0	10.0 %	110	125	106	17.5
12.5 %	−1.67	3.18	2.54	−123	12.5 %	129	143	125	12.9
15.0 %	−10.3	−3.17	−7.44	−160	15.0 %	146	160	148	11.7
U _W E _T R	BORB	EORB	NORB	AORB	U _N E _T R	BORB	EORB	NORB	AORB
5.0 %	106	113	111	37.2	5.0 %	77.3	79.4	70.9	27.7
7.5 %	123	132	129	25.6	7.5 %	97.3	97.3	86.7	24.2
10.0 %	144	155	148	6.77	10.0 %	116	119	103	17.9
12.5 %	163	176	169	−9.74	12.5 %	135	138	118	12.8
15.0 %	184	192	185	−23.3	15.0 %	154	153	130	9.05

Table 7

Diagonal energy-based restoration percentages of rejuvenated bitumen.

E _D R	BORB	EORB	NORB	AORB	U _V E _D R	BORB	EORB	NORB	AORB
5.0 %	56.7	90.2	93.5	−145	5.0 %	294	342	308	49.8
7.5 %	57.9	108	82.6	−233	7.5 %	402	474	430	20.6
10.0 %	34.8	86.2	76.2	−383	10.0 %	493	598	517	2.44
12.5 %	13.3	78.3	68.4	−522	12.5 %	596	712	624	−14.1
15.0 %	6.11	98.1	68.1	−687	15.0 %	701	828	762	−47.2
U _W E _D R	BORB	EORB	NORB	AORB	U _N E _D R	BORB	EORB	NORB	AORB
5.0 %	−301	−358	−358	−30.6	5.0 %	198	221	199	36.6
7.5 %	−433	−485	−460	0.34	7.5 %	292	302	263	30.4
10.0 %	−494	−582	−563	70.5	10.0 %	341	373	325	9.78
12.5 %	−584	−691	−659	123	12.5 %	407	446	382	−3.16
15.0 %	−687	−804	−760	205	15.0 %	477	512	440	−30.1

Table 8

Cross-terms energy-based restoration percentages of rejuvenated bitumen.

E _{CT} R	BORB	EORB	NORB	AORB	U _V E _{CT} R	BORB	EORB	NORB	AORB
5.0 %	6.55	4.33	2.34	4.67	5.0 %	−2.69	−5.05	−5.38	2.35
7.5 %	6.76	6.81	4.67	11.9	7.5 %	−6.90	−7.40	−8.75	−0.59
10.0 %	11.6	7.58	5.95	15.4	10.0 %	−7.49	−13.0	−11.4	−3.36
12.5 %	14.6	9.44	9.14	19.5	12.5 %	−10.3	−14.1	−13.5	−4.96
15.0 %	17.8	12.4	11.8	24.9	15.0 %	−12.5	−20.6	−17.2	−5.80
U _W E _{CT} R	BORB	EORB	NORB	AORB	U _N E _{CT} R	BORB	EORB	NORB	AORB
5.0 %	−0.65	−2.74	−4.22	0.23	5.0 %	−5.14	−7.27	−7.37	−1.92
7.5 %	−3.34	−3.76	−5.85	−0.93	7.5 %	−12.0	−10.2	−10.5	−4.11
10.0 %	−4.36	−7.06	−8.22	−1.53	10.0 %	−12.5	−16.1	−14.4	−5.10
12.5 %	−4.83	−9.38	−9.01	−2.14	12.5 %	−16.2	−20.3	−16.3	−5.55
15.0 %	−5.94	−12.0	−10.1	−2.97	15.0 %	−19.4	−24.7	−18.5	−7.04

Table 9

Effects of aging and adding RAs on different energy parameters of bitumen.

Energy parameters	E _p	E _k	E _N	E _T	E _D	E _{CT}
E	Aging Adding RAs	+	−	+	+	+
—	—	−	+	−	+	+
—	—	+(AO)	—	—	+(BO, AO)	—
U _V E	Aging Adding RAs	+	−	+	+	+
—	—	−	−	−	−	−
—	—	+(AO)	+(AO)	+(AO)	−, +(AO)	+
U _W E	Aging Adding RAs	+	−	+	+	+
—	—	−	+	−	O*	+
—	—	+(AO)	+(AO)	+(AO)	−, +(AO)	+
U _N E	Aging Adding RAs	+	−	+	+	+
—	—	−	−	−	−	−
—	—	+(AO)	+(AO)	+(AO)	−, +(AO)	+

Note: “+” and “−” mean the increasing effect and decreasing effect, respectively.
O* shows no variation law.

effect of all RAs on atomic-level energy characteristics of aged bitumen, except for the U_NE_D and U_VE_P parameters in aromatic-oil rejuvenated bitumen cases. The effects of recycling agent on various critical energy parameters are different. For bio-oil, engine-oil, and naphthenic-oil, their influence levels on these energy parameters follow the sequence of U_NE_D > U_VE_P > U_VE_T > U_WE_K > E_N > E_{CT}. Thus, the restoration efficiency is affected not only by molecular type/dosage, but also the model size (entire, per volume, per weight, or per molecule). For aromatic-oil rejuvenated bitumen, the E_{CT}R, U_VE_T, E_N, and U_WE_K values are all lower than 25 %, indicating that the aromatic-oil has a limited recovery potential on these critical energy indices of aged bitumen. It is anticipated that these pivotal energy indicators will be applicable to assess the restorat efficiency in other cases of RAs, requiring further validation and optimization. Moreover, these fundamental energy parameters of virgin, aged, and rejuvenated binders will be correlated with their respective critical high-temperature indicators from experiments to establish a multi-scale evaluation framework for assessing the restoration efficiency of RAs on aged bitumen properties.

The critical energy parameter-based restoration percentages of rejuvenated bitumen are displayed in Fig. 6 with variable recycling agent (RA) types and dosages. All energy restoration percentages show linear relationships with RA content. Apart from the U_VE_PR, U_VE_TR, and

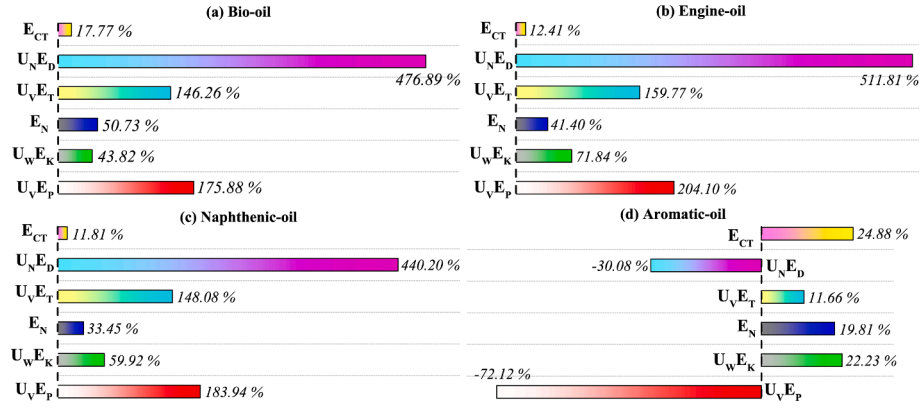


Fig. 5. Comparison in energy parameter-based restoration percentages of rejuvenated bitumen.

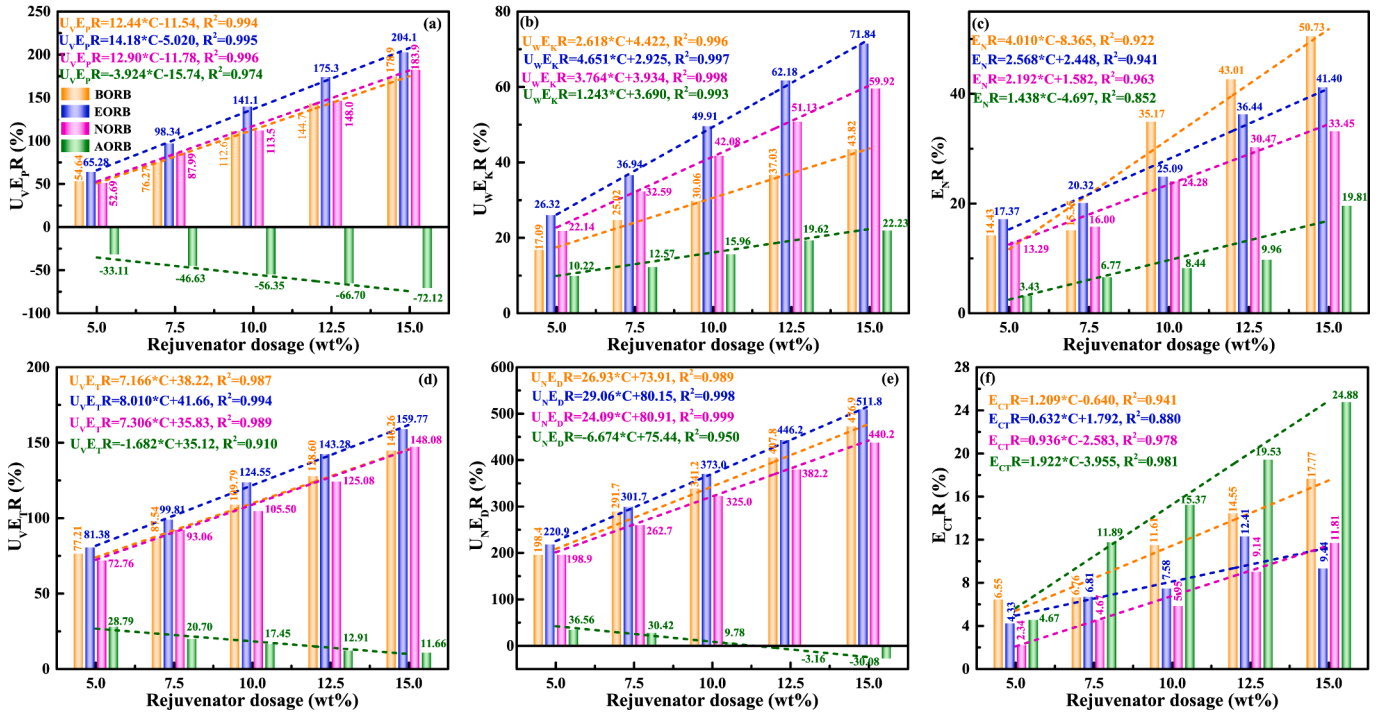


Fig. 6. Critical energy parameter-based restoration percentages of rejuvenated bitumen.

$U_N E_D R$ values of AORB, the increased RA dosage promotes the increment in energy restoration percentages of all rejuvenated binders. Moreover, the restoration percentages and their responsiveness to RA dosage are significantly influenced by the RA type. Among them, the engine-oil demonstrates the most substantial recovery efficiency on potential, kinetic, total, and diagonal energies of aged bitumen, followed by naphthenic-oil and bio-oils, while aromatic-oil exhibits the least impact on these energy parameters. Additionally, the bio-oil exhibits the highest recovery efficacy on non-bond energy, followed by engine-oil, naphthenic-oil, and aromatic-oil. These findings agree well with the experimental conclusion that bio-oil and engine-oil show the highest restoration percentages on high-temperature performance recovery of aged bitumen, followed by naphthenic-oil, whereas the aromatic-oil preserves the high-temperature rutting resistance of aged bitumen to the greatest extent [23]. Nevertheless, it is observed that none of these crucial energy parameters exhibit the same restoration percentage as those derived from experimentally measured mechanical indicators. This observation indicates that the macroscale performance of rejuvenated bitumen is the result of collective influence of molecular-scale

energy parameters.

Interestingly, the magnitude of $E_N R$ values of rejuvenated bitumen is the same as the order of restoration percentages based on critical high-temperature indicators (BORB > EORB > NORB > AORB). It is speculated that the non-bond energy recovery may be the key restoration mechanism of these recycling agents (RAs), which still needs to be further studied and verified. Moreover, the aromatic-oil shows the highest restoration effectiveness on cross-terms energy of aged bitumen, which is opposite to the experimental indicators. Therefore, the impact of cross-terms energy on the macroscale high-temperature properties of rejuvenated bitumen might be less prominent.

5. High-temperature rheological properties of rejuvenated bitumen

Based on the findings from previous work [24], the critical indicators for effectively evaluating restoration levels of these recycling agents on high-temperature performance of aged bitumen are rutting failure temperature (RFT), zero-shear viscosity (ZSV), recovery percentage

($R_{3,2}$), and creep compliance ($J_{nr3,2}$) at the stress level of 3.2 kPa. Their sensitivities to ρ , CED, Ds, U_{VEp} , U_{WEK} , E_N , U_{VET} , U_{NED} , and E_{CT} will be analysed and compared. The critical high-temperature parameters of rejuvenated binders are listed in Table 10. As the long-term aging deepens, the RFT, ZSV, and $R_{3,2}$ values of bitumen enlarge significantly, whereas the $J_{nr3,2}$ value reduces. It implies that the high-temperature rutting and deformation resistance of bitumen enlarges during the long-term aging process. The incorporation of a recycling agent (RA) restores all critical high-temperature indicators of aged bitumen, which enlarges as the RA dosage increases. To build a multi-scale evaluation framework on high-temperature performance of rejuvenated bitumen, these critical high-temperature indicators will be connected with thermodynamic and energy parameters outputted from MD simulations.

6. Correlation explorations and further discussion

6.1. Rheological properties and cohesive energy density (CED)

Different critical high-temperature performance indicators of all bitumen are connected with predicted CED values, shown in Fig. 7. The variation trends of RFT-CED, ZSV-CED, $R_{3,2}$ -CED, and $J_{nr3,2}$ -CED curves are similar to their correlation curves with density. It implies that the CED parameter of bitumen is positively linked with high-temperature rutting resistance. Regarding the correlation level, the CED parameter is slightly worse than the ρ index according to the lower R^2 values. In addition, the ZSV index still has the best association effect with predicted CED values than the other critical measurement parameters. The ranking for the sensitivity level of these critical indicators to CED is the same as ρ case ($R_{3,2} > RFT > \log(J_{nr3,2}) > \log(ZSV)$). Hence, the high-temperature deformation characteristics of bituminous materials are closely tied to the level of intermolecular interaction, where a higher CED value signifies increased rutting resistance in bitumen. Although both ρ and CED indices exhibit strong correlations with high-

temperature properties, they offer distinct insights at the atomic level. The density index reflects the overall compactness of the bitumen model, capturing intermolecular forces and distances. On the other hand, the CED index encapsulates intermolecular interactions from an energy perspective. Consequently, the density parameter proves more accurate in predicting high-temperature critical rheo-mechanical properties compared to the CED index.

6.2. Rheological properties and energy parameters

The CED results reveal that the intermolecular interaction (energy) is significantly attributed to these critical high-temperature indicators of rejuvenated bitumen. At the atomic level, the interaction energy of the bitumen model is composed of different terms, and their contributions to high-temperature performance are still unclear. Therefore, this subsection aims at exploring and comparing the links between various effective energy parameters (U_{VEp} , U_{WEK} , E_N , U_{VET} , U_{NED} , and E_{CT}) and critical high-temperature indicators, and further optimizing the essential energy parameter for both assessing the recovery level and predicting the macroscale properties of virgin/aged and rejuvenated bitumen.

6.2.1. Potential, total, and diagonal energy

Fig. 8 depicts the correlation curves between U_{VEp} and RFT, ZSV, $R_{3,2}$, and $J_{nr3,2}$ indicators of rejuvenated bitumen. All correlation curves of the AORB binder show the opposite trends to the others because the potential energy fails to evaluate the restoration effect of the aromatic-oil. Apart from AORB binders, the RFT, ZSV, and $R_{3,2}$ indices increase linearly, while the $J_{nr3,2}$ tends to decline as the increment in U_{VEp} value. It means that the potential energy contributes positively to the high-temperature performance of bitumen. Based on the R^2 values of correlation equations, the correlation levels of RFT- U_{VEp} , ZSV- U_{VEp} , $R_{3,2}$ - U_{VEp} , and $J_{nr3,2}$ - U_{VEp} curves are between 0.70–0.81, which are similar to the CED but lower than ρ parameter. In addition, the correlation level of the AORB binder is lower than the others. Similar to ρ and CED cases, the ZSV index shows the highest correlation level with potential energy, followed by RFT, while the $R_{3,2}$ and $J_{nr3,2}$ from multiple stress creep and recovery (MSCR) tests show lower R^2 values. In a word, potential energy strongly affects the high-temperature rutting performance of bitumen with a high correlation coefficient. However, this correlation law does not match the aromatic-oil rejuvenated bitumen case, which needs to be considered separately.

6.2.2. Kinetic energy

The correlation curves and corresponding equations between the kinetic energy parameter U_{WEK} and four critical indicators are illustrated in Fig. 9. The variation trends of RFT- U_{WEK} , ZSV- U_{WEK} , $R_{3,2}$ - U_{WEK} , and $J_{nr3,2}$ - U_{WEK} are the same as the self-diffusion coefficient (D_s) case because the kinetic energy is the basic of the molecular mobility of bitumen molecules. Nevertheless, the kinetic energy presents great correlations with the macroscale properties with high correlation coefficient R^2 values higher than 0.8. As the U_{WEK} value rises, the RFT, $\log(ZSV)$, and $R_{3,2}$ values of virgin/aged and rejuvenated bitumen decline linearly, while the $\log(J_{nr3,2})$ index increases linearly. It manifests that the bitumen with a lower kinetic energy would exhibit a greater high-temperature rutting resistance. It is essential to highlight that the correlation pattern between kinetic energy and macroscale indicators is applicable to all recycling agent cases, in contrast to potential energy. Therefore, the kinetic energy term can succeed in predicting the RFT, ZSV, $R_{3,2}$, and $J_{nr3,2}$ indicators for evaluating and comparing the recovery levels of various recycling agents on the high-temperature performance of rejuvenated bitumen. Based on the absolute slope values, the influence level of the $R_{3,2}$ index to U_{WEK} value is the largest, followed by the RFT, while the ZSV and $J_{nr3,2}$ parameters are similar. Interestingly, the ZSV index still connects greatest to kinetic energy than others, which is also observed in ρ , CED, and U_{VEp} cases.

Table 10
Critical high-temperature indicators of rejuvenated bitumen.

Samples	RFT (°C)	ZSV (kPa·s)	$R_{3,2}$ (%)	$J_{nr3,2}$ (kPa ⁻¹)
VB	64.51	316.3	0.12	2.41
SAB	69.00	721.9	3.86	0.85
1P	80.00	336.3	18.8	0.48
2P	87.00	8496	50.1	0.03
4P	105.0	68,200	65.7	0.02
1P10B	65.35	451.1	0.74	2.50
1P10E	66.94	499.5	2.38	1.87
1P10N	69.30	710.8	3.84	1.24
1P10A	71.59	978.4	6.91	0.79
2P5B	79.04	3014	26.4	0.23
2P7.5B	76.37	2094	19.1	0.39
2P10B	72.30	1081	8.56	0.84
2P12.5B	70.40	773.0	5.50	1.23
2P15B	67.31	487.4	2.90	1.98
2P5E	79.84	4380	30.2	0.18
2P7.5E	76.26	2171	21.4	0.34
2P10E	73.87	1261	14.7	0.56
2P12.5E	71.22	1083	9.09	0.91
2P15E	68.85	598.3	4.83	1.44
2P5N	79.45	4509	30.3	0.18
2P7.5N	77.08	2456	23.4	0.29
2P10N	74.51	1524	16.5	0.48
2P12.5N	72.10	1038	9.57	0.75
2P15N	70.02	767.8	6.87	1.10
2P5A	81.29	5373	32.3	0.13
2P7.5A	79.47	3903	27.1	0.18
2P10A	77.24	2351	20.4	0.28
2P12.5A	75.05	1754	14.4	0.43
2P15A	73.33	1324	10.0	0.59
4P10B	83.89	9052	49.4	0.10
4P10E	84.73	11,799	55.1	0.06
4P10N	86.96	15,075	62.4	0.04
4P10A	85.76	10,996	49.1	0.05

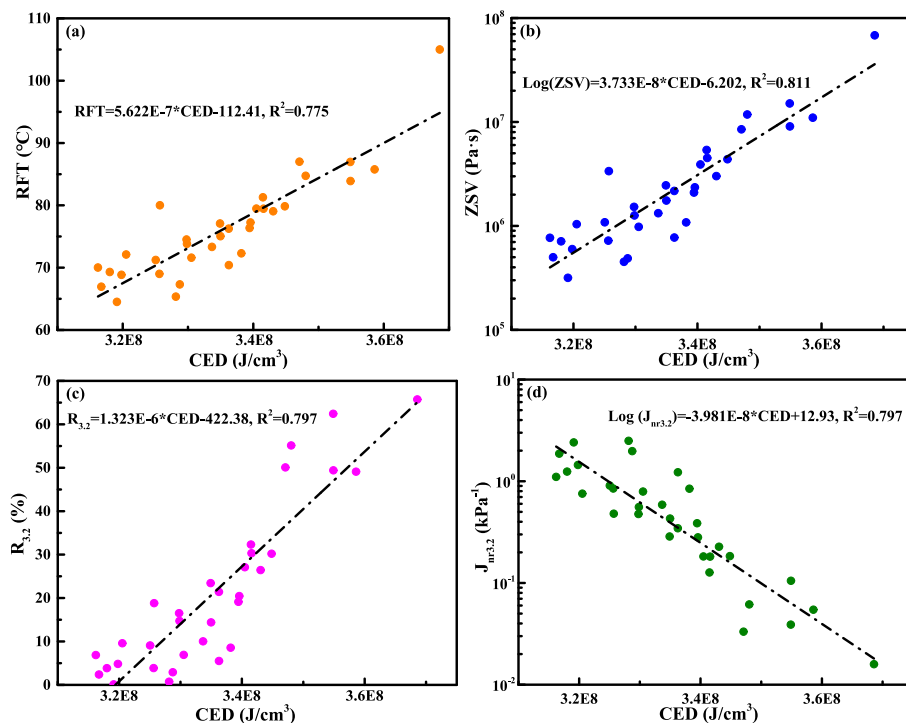


Fig. 7. Correlations between high-temperature critical parameters with CED.

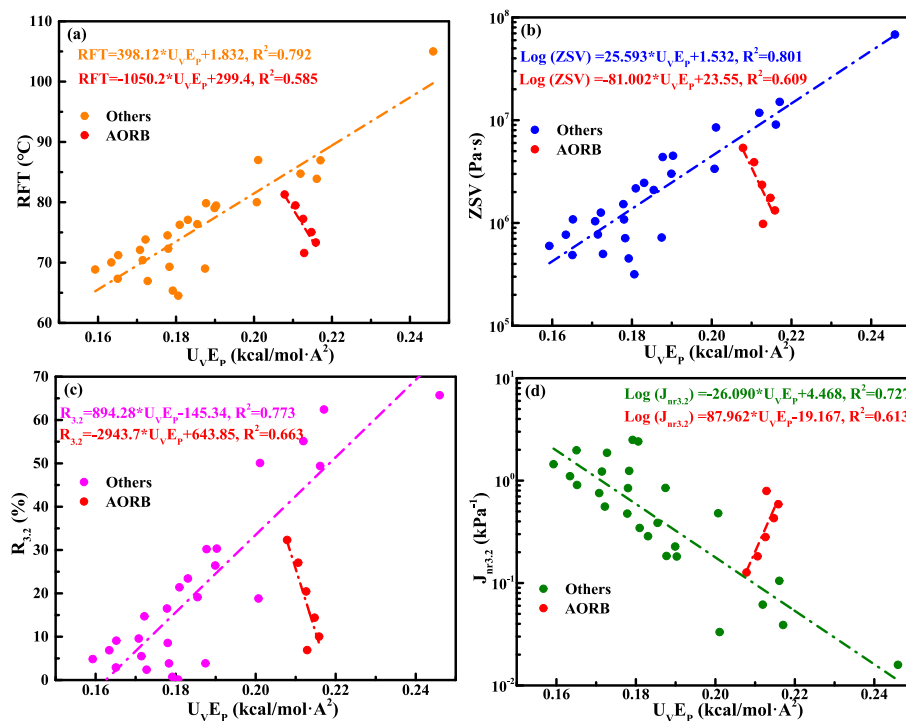


Fig. 8. Correlations between high-temperature critical parameters with potential energy.

6.2.3. Non-bond and cross-terms energy

From the viewpoint of intermolecular interaction, the macroscale deformation at high temperatures of material is mainly associated with the non-bond energy without chemical reaction (bond breaking and formation). Non-bond energy is composed of van der Waals energy, electrostatic energy, and hydrogen energy. The difference in molecular components would change these energy elements, while only the whole

non-bond energy is considered in this study. Fig. 10 probes the potential relationships between the non-bond energy and critical indicators from experiments. Dissimilar to potential and kinetic energy, the correlation law of RFT- E_N , ZSV- E_N , $R_{3,2}$ - E_N , and $J_{nr3,2}$ - E_N curves are strongly dependent on the aging degree of bitumen. As the aging level deepens, the correlation curves of RFT- E_N , ZSV- E_N , and $R_{3,2}$ - E_N move to the upper right, while the $J_{nr3,2}$ - E_N curve tends to the bottom right. Therefore, the

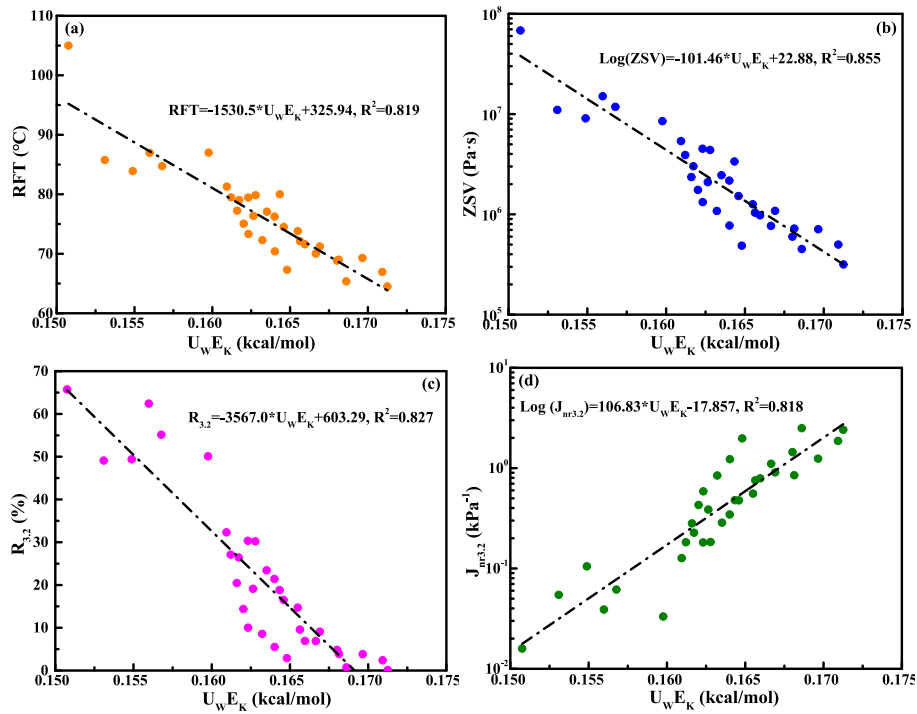


Fig. 9. Correlations between high-temperature critical parameters and kinetic energy.

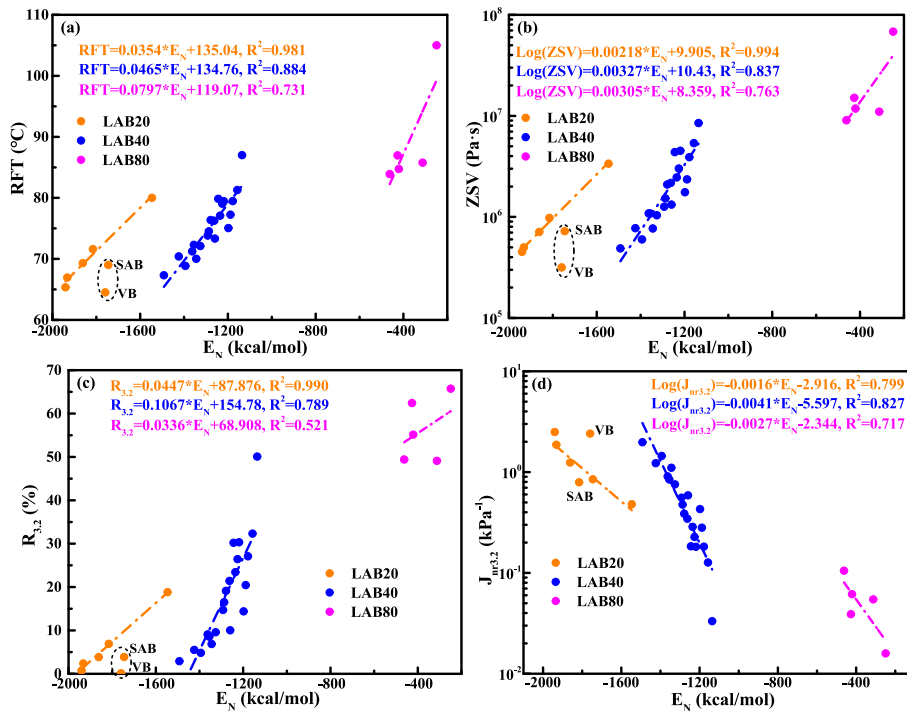


Fig. 10. Correlations between high-temperature critical parameters and non-bond energy.

general correlation law bridging the non-bond energy with macroscale indicators of various rejuvenated bitumen cannot be derived due to the large dependence on the aging level.

However, the linear correlations of rejuvenated bitumen with the same aging degree are observed. As the non-bond energy (E_N) rises, the RFT, $\text{Log}(ZSV)$, and $R_{3.2}$ values enlarge linearly, whereas the $\text{Log}(J_{nr3.2})$ decreases, indicating that the non-bond energy term is positively connected with high-temperature rutting resistance of bitumen. Thus, the

projected E_N values can serve as predictors for macroscale indicators, but it is important to explicitly consider the aging degree of bitumen. Notably, the data points for VB and SAB binders fall outside any correlation curves for rejuvenated bitumen due to variations in aging levels.

In summary, all energy parameters play a role in influencing the high-temperature performance of bituminous materials, with most exhibiting positive correlations with rutting resistance, except for the kinetic energy term. The potential energy, total energy, and diagonal

energy display similar correlation trends with critical indicators, while bitumen rejuvenated with aromatic oil shows the opposite trend and should be excluded. Additionally, kinetic energy aligns well with macroscale indices. Regarding non-bond energy and cross-terms energy, correlation curves are significantly influenced by the aging degree of bitumen. Predictions of high-temperature properties in rejuvenated bitumen with a specific aging degree can be accomplished using non-bond energy, in contrast to cross-terms energy, which exhibits poor correlation levels. Consequently, the kinetic energy term is considered the primary choice as a crucial energy index for predicting high-temperature critical indicators across various rejuvenated bitumen formulations.

It was reported that aromatic molecules have a beneficial impact on restoring the molecular conformation of aged bitumen [30]. This effect is ascribed to the presence of the polar aromatic motif in aromatic-oil, which readily disrupts the asphaltene stack via π - π stacking interactions. In addition, bio-oil and naphthenic-oil were identified as more effective recycling agents in comparison to engine-oil. The polar ester functional group in bio-oil weakens π - π interactions between asphaltene sheets, distinguishing it from the less polar naphthenic-oil and saturated engine-oil [31]. It was also revealed that the predominant volatiles consist of single-ring aromatics with short side chains, followed by saturated and unsaturated aliphatic compounds. Thus, more attention should be paid on the mass loss and emission potential of engine-oil. Drawing from the literature [30–32], it is inferred that attaining both short-term and long-term rejuvenation efficacy requires striking a balance in chemical components and restoring molecular conformation.

7. Conclusions and recommendations

This study employs molecular dynamics simulations to explore the combined effects of recycling agent (RA) type, dosage, and bitumen aging degree on the energy parameters of aged bitumen. These energy parameters are correlated with rheological indices to predict the high-temperature performance of rejuvenated bitumen. The main findings are summarized as follows:

- (1) All recycling agents (RAs) can bring the cohesive energy density of aged bitumen closer to that of virgin bitumen, with temperature having a more pronounced effect than RA dosage. The increment in the aging level of bitumen weakens the recovery degree, and no recycling agent fully restores it to the virgin bitumen level.
- (2) The U_{VEP} , U_{WEK} , E_N , U_{VET} , U_{NED} , and E_{CT} indices can reflect the restoration level of recycling agents on the atomic-level energy components of aged bitumen. Engine-oil stands out in restoration potential on kinetic, total, and diagonal energies of aged bitumen, followed by naphthenic-oil, bio-oil, and aromatic-oil. Moreover, bio-oil presents the highest restoration efficacy on non-bond energy with the same order of restoration percentages based on critical high-temperature indicators (BORB > EORB > NORB > AORB).
- (3) The CED parameters link to the high-temperature rheological and mechanical properties of rejuvenated bitumen well. Compared to RFT, $R_{3.2}$, and $J_{nr3.2}$, the ZSV index of bitumen greatly correlates with the predicted ρ and CED values.
- (4) All energy parameters positively correlate with rutting resistance, except for kinetic energy. The potential energy, total energy, and diagonal energy of rejuvenated bitumen display similar correlation trends, with the exception of aromatic oil case. Kinetic energy always aligns well with macroscale indices, but both non-bond energy and cross-terms energy correlations are strongly influenced by bitumen aging. Utilizing kinetic energy is suggested as a means to predict the high-temperature rheological performance of rejuvenated bitumen.

In the future, greater focus will be dedicated to evaluating the energy recovery mechanism to determine the suitability of these suggested MD indicators in distinguishing between softeners and rejuvenators. Moreover, the influence of these RAs on the adhesion performance and moisture susceptibility related to durability will be studied. Importantly, the variation in molecular structures of bitumen after adding RAs and their blending degree will be explored by using DFT method, especially for the asphaltene deagglomeration (self-assembly) potential [30–34]. Only in way can we differentiate softeners from real rejuvenators [35,36]. Lastly, more advanced data analysis method (such as machine learning) will be developed to connect the thermodynamic parameters with macroscale rheological indices accurately.

CRediT authorship contribution statement

Shisong Ren: Writing – original draft, Validation, Resources, Methodology, Investigation, Formal analysis, Data curation. **Xueyan Liu:** Writing – review & editing, Supervision, Resources. **Sandra Erkens:** Writing – review & editing, Supervision.

Declaration of competing interest

The authors declare that they have no known competing financial interests or personal relationships that could have appeared to influence the work reported in this paper.

Data availability

Data will be made available on request.

Acknowledgment

The first author would thank the China Scholarship Council for the funding support (CSC, No.201906450025).

Appendix A. Supplementary data

Supplementary data to this article can be found online at <https://doi.org/10.1016/j.matdes.2024.112957>.

References

- [1] Road Pavement Transition Path. <https://www.duurzame-infra.nl/roadmaps-uitvoering/transitiepad-wegverharding>.
- [2] Towards climate-neutral and circular government infrastructure projects. Ministry of Infrastructure and Water Management. <https://www.duurzame-infra.nl>.
- [3] A. Rajib, A. Samieadel, A. Zalghout, K. Kaloush, B. Sharma, E. Fini, Do all rejuvenators improve asphalt performance? Road Materials and Pavement Design 23 (2) (2022) 358–376.
- [4] X. Yang, H. Zhang, W. Zheng, Z. Chen, C. Shi, A novel rejuvenating method for structural and performance recovery of aged SBS-modified bitumen, ACS Sustain. Chem. Eng. 10 (4) (2022) 1565–1577.
- [5] E. Fini, A. Rajib, D. Oldham, A. Samieadel, S. Hosseinneshad, Role of chemical composition of recycling agents in their interaction with oxidized asphaltene molecules, J. Mater. Civ. Eng. 32 (9) (2020) 04020268.
- [6] R. Moraes, F. Yin, C. Rodezno, Laboratory performance and compositional evaluation of bio-based recycling agents, Transp. Res. Rec. 1–13 (2023).
- [7] E. Bocci, E. Prosperi, P. Marsac, Evolution of rheological parameters and apparent molecular weight distribution in the bitumen from reclaimed asphalt with rejuvenation and re-ageing, Road Mater. Pavement Design 23 (S1) (2022) S16–S35.
- [8] S. Shariati, S. Aldagari, E. Fini, Bio-modifier: a sustainable suturing technology at the bitumen-aggregate interface, ACS Sustain. Chem. Eng. 11 (24) (2023) 8908–8915.
- [9] A. Rajib, Structure-property relationships to understand comprehensive rejuvenation mechanisms of aged asphalt binder, Doctoral Dissertation (2020).
- [10] H. Yu, J. Ge, G. Qian, C. Zhang, W. Dai, P. Li, Evaluation on the rejuvenation and diffusion characteristics of waste cooking oil on aged SBS asphalt based on molecular dynamics method, J. Clean. Prod. 406 (2023) 136998.
- [11] B. Cui, X. Gu, D. Hu, Q. Dong, A multiphysics evaluation of the rejuvenator effects on aged asphalt using molecular dynamics simulations, J. Clean. Prod. 259 (2020) 120629.

- [12] X. Zhang, X. Zhou, L. Chen, F. Lu, F. Zhang, Effects of poly-sulfide regenerant on the rejuvenated performance of SBS modified asphalt-binder, *Mol. Simul.* 47 (17) (2021) 1423–1432.
- [13] X. Qu, D. Wang, Y. Hou, M. Oeser, L. Wang, Influence of paraffin on the microproperties of asphalt binder using MD simulation, *J. Mater. Civ. Eng.* 30 (8) (2018) 04018191.
- [14] H. Ding, H. Wang, X. Qu, A. Varveri, J. Gao, Z. You, Towards an understanding of diffusion mechanism of bio-rejuvenators in aged asphalt binder through molecular dynamics simulation, *J. Clean. Prod.* 299 (2021) 126927.
- [15] S. Yan, Q. Dong, X. Chen, X. Zhao, X. Wang, Performance evaluation of waste cooking oil at different stages and rejuvenation effect of aged asphalt through molecular dynamics simulations and density functional theory calculations, *Constr. Build. Mater.* 350 (2022) 128853.
- [16] C. Bao, C. Zheng, Y. Xu, L. Nie, Y. Wang, Role of rejuvenator properties in determining the activation effects on aged asphalt based on molecular simulations, *J. Clean. Prod.* 405 (2023) 136970.
- [17] K. Sonibare, G. Rucker, L. Zhang, Molecular dynamics simulation on vegetable oil modified model asphalt, *Constr. Build. Mater.* 270 (2021) 121687.
- [18] M. Zadshtir, D. Oldham, S. Hosseinneshad, E. Fini, Investigating bio-rejuvenation mechanisms in asphalt binder via laboratory experiments and molecular dynamics simulation, *Constr. Build. Mater.* 190 (2018) 392–402.
- [19] X. Zhang, Y. Ning, X. Zhou, X. Xu, X. Chen, Quantifying the rejuvenation effects of soybean-oil on aged asphalt-binder using molecular dynamics simulations, *J. Clean. Prod.* 317 (2021) 128375.
- [20] M. Gong, B. Jiao, Thermodynamic properties analysis of warm-mix recycled asphalt binders using molecular dynamics simulation, *Road Materials and Pavement Design* (2023) 2199883.
- [21] E. Fini, A. Samieadel, A. Rajib, Moisture damage and its relation to surface adsorption/desorption of rejuvenators, *Ind. Eng. Chem. Res.* 59 (2020) 13414–13419.
- [22] D. Li, Y. Ding, J. Wang, Y. Shi, Z. Cao, G. Sun, B. Huang, Multiscale molecular simulations on the rejuvenation of recycled asphalt mixture: an insight into molecular impact of rejuvenators in aged binders, *J. Clean. Prod.* 414 (2023) 137621.
- [23] G. Xu, Y. Yao, T. Ma, S. Hao, B. Ni, Experimental study and molecular simulation on regeneration feasibility of high-content waste tire crumb rubber modified asphalt, *Constr. Build. Mater.* 369 (2023) 130570.
- [24] S. Ren, X. Liu, S. Erkens, Unraveling the critical indicators for evaluating the high-temperature performance of rejuvenator-aged bitumen blends. *Case Studies in Construction Materials*. Revision submitted.
- [25] S. Ren, X. Liu, P. Lin, S. Erkens, Y. Xiao, Chemo-physical characterization and molecular dynamics simulation of long-term aging behaviors of bitumen, *Constr. Build. Mater.* 302 (2021) 124437.
- [26] A. Rajib, F. Pahlavan, E. Fini, Investigating molecular-level factors that affect the durability of restored aged asphalt binder, *J. Clean. Prod.* 270 (2020) 122501.
- [27] M. Mousavi, F. Pahlavan, D. Oldham, S. Hosseinneshad, E. Fini, Multiscale investigation of oxidative aging in biomodified asphalt binder, *J. Phys. Chem. C* 120 (2016) 17224–17233.
- [28] S. Ren, X. Liu, P. Lin, S. Erkens, Y. Gao, Chemical characterizations and molecular dynamics simulations on different rejuvenators for aged bitumen recycling, 2022, *Fuel*. 324, Part A, 124550.
- [29] F. Pahlavan, A. Rajib, S. Deng, P. Lammers, E. Fini, Investigation of balanced feedstocks of lipids and proteins to synthesize highly effective rejuvenators for oxidized asphalt, *ACS Sustain. Chem. Eng.* 8 (2020) 7656–7667.
- [30] F. Pahlavan, S. Hosseinneshad, A. Samieadel, A. Hung, E. Fini, Fused aromatics to restore molecular packing of aged bituminous materials, *Ind. Eng. Chem. Res.* 58 (2019) 11939–11953.
- [31] M. Mousavi, S. Aldagari, E. Fini, Adsorbing volatile organic compounds within bitumen improves colloidal stability and air quality, *ACS Sustain. Chem. Eng.* 11 (2023) 9581–9594.
- [32] A. Hung, F. Pahlavan, S. Shakiba, S. Chang, S. Louie, E. Fini, Preventing assembly and crystallization of alkane acids at the silica-bitumen interface to enhance interfacial resistance to moisture damage, *Ind. Eng. Chem. Res.* 58 (2019) 21542–21552.
- [33] P. Hajikarimi, S. Shariati, M. Rahi, R. Kazemi, F. Nejad, E. Fini, Enhancing the economics and environmental sustainability of the manufacturing process for air blown bitumen, *J. Clean. Prod.* 323 (2021) 128978.
- [34] S. Shariati, A. Rajib, E. Fini, A multifunctional bio-agent for extraction of aged bitumen from siliceous surfaces, *J. Ind. Eng. Chem.* 104 (2021) 500–513.
- [35] A. Samieadel, E. Fini, Interplay between wax and polyphosphoric acid and its effect on bitumen thermomechanical properties, *Constr. Build. Mater.* 243 (2020) 118194.
- [36] Q. Ye, Z. Yang, S. Lv, J. Jin, S. Zhang, Study on components selection and performance of bio-oil based asphalt rejuvenator based on softening and asphaltene deagglomeration effect, *J. Clean. Prod.* 419 (2023) 138238.